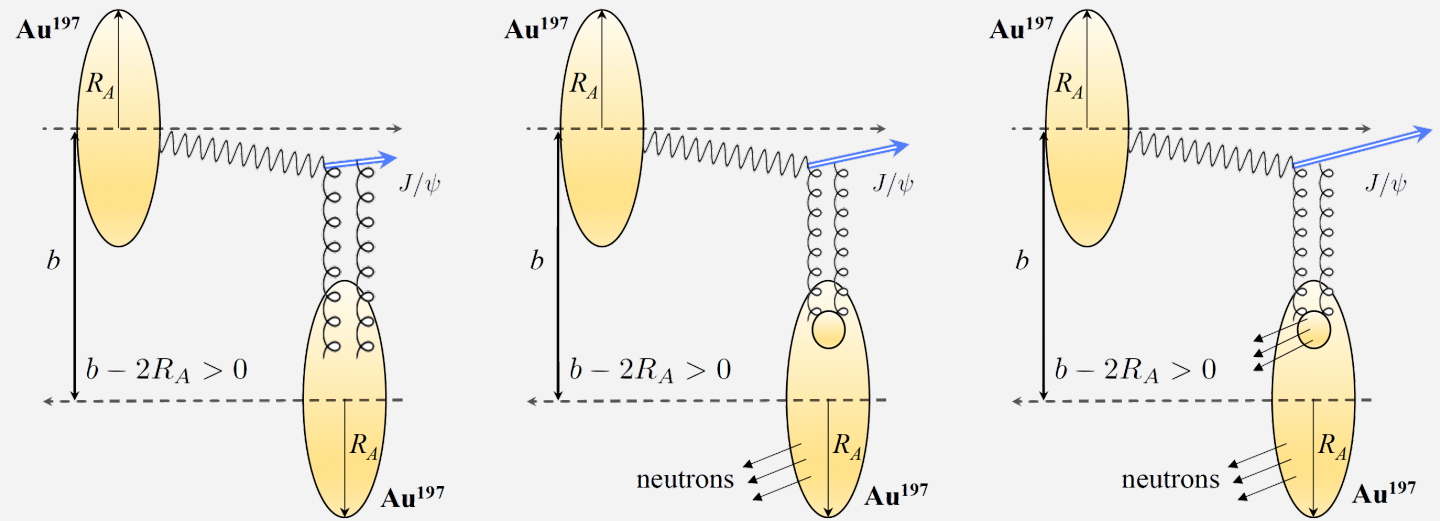




Probing nuclear parton density and fluctuation with ultra-peripheral collisions at RHIC



Kong Tu (BNL)

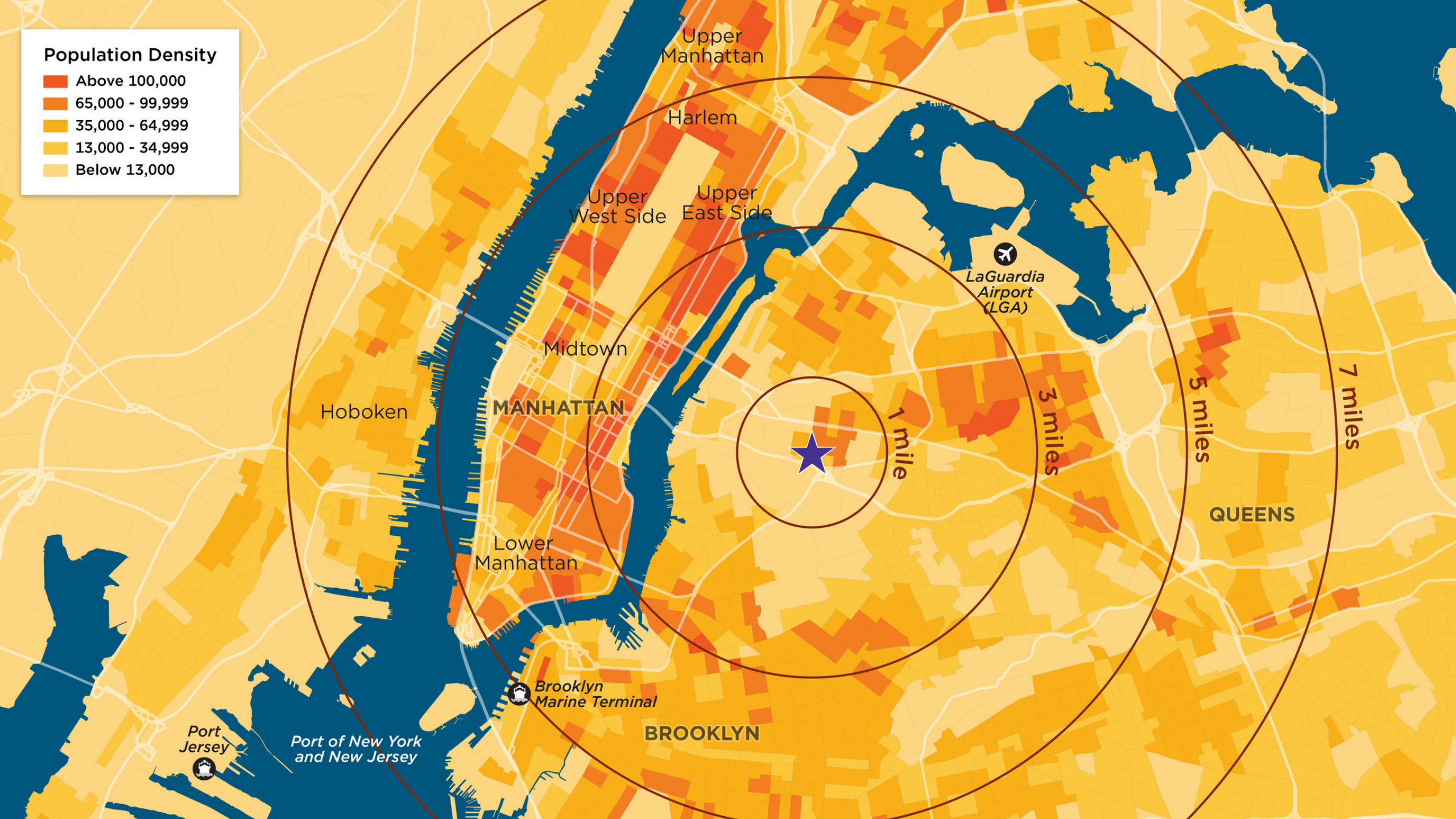
(a) Coherent with nucleus stays intact

(b) Incoherent with elastic nucleon

(c) Incoherent with nucleon dissociative

Population Density

- Above 100,000
- 65,000 - 99,999
- 35,000 - 64,999
- 13,000 - 34,999
- Below 13,000





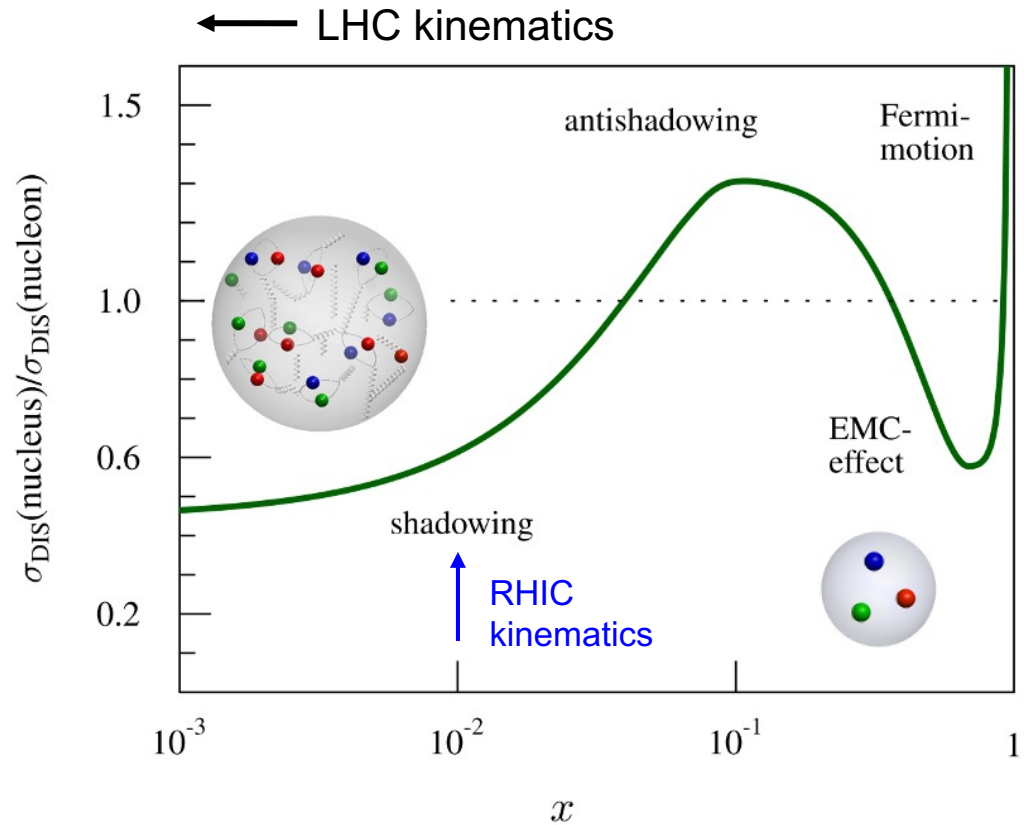
Average density and its day-by-day, hour-by-hour fluctuation are two distinct aspects of describing the Manhattan's populations

Together, we have a **full picture of the structure**



Motivation

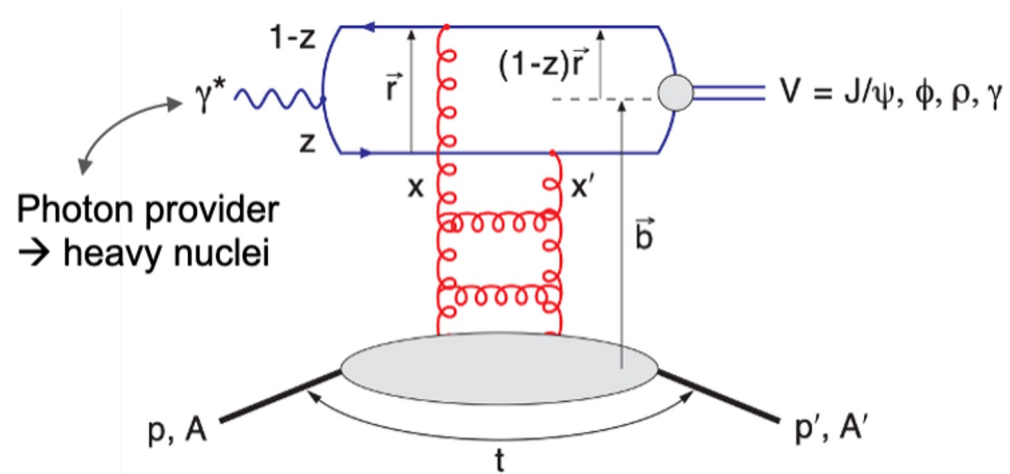
- Physics mechanism of **modified parton densities** in heavy nuclei - one of the most pressing questions in both **hot and cold QCD community**.
- Photoproduction of Vector Mesons, e.g., J/ψ , is considered a **clean probe** to the nuclear parton structures.





J/ψ photoproduction

At Leading Order, 2-gluon exchange

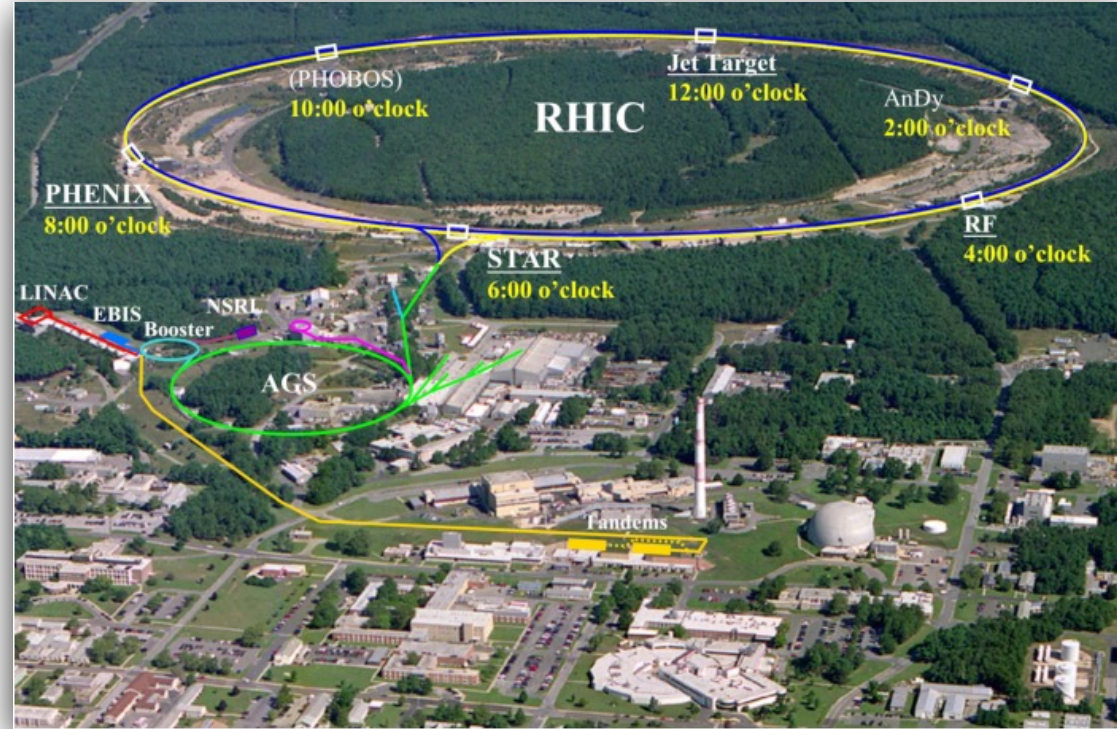
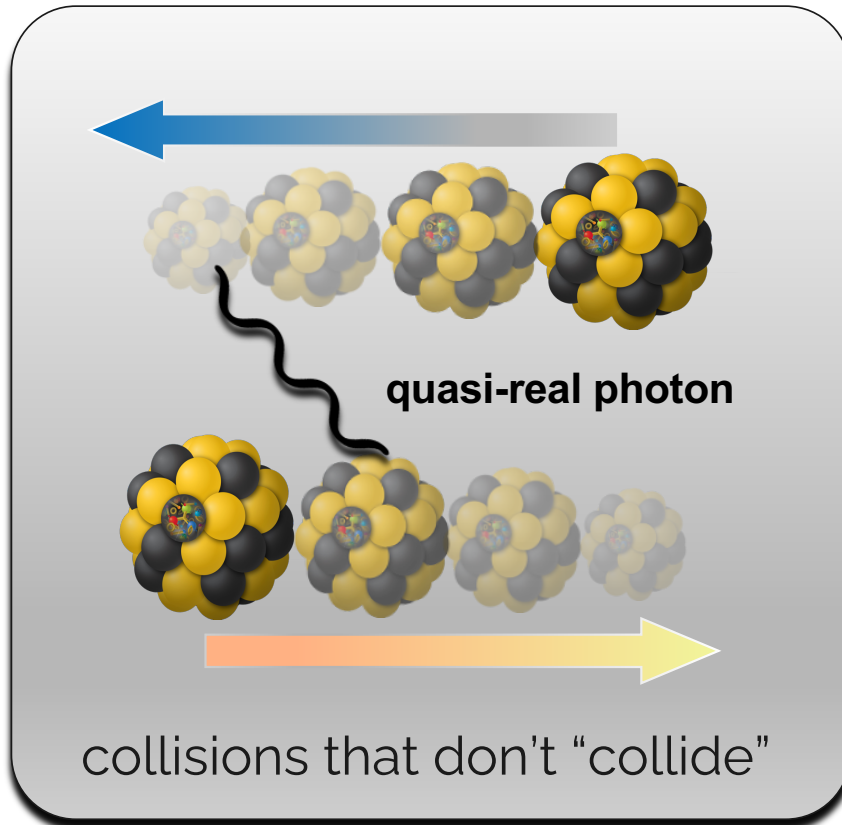


Coherent (target stays intact)	Incoherent (target breaks up)
Average nuclear parton density	Event-by-event parton density fluctuations
Momentum transfer (t) and transverse spatial position (b) are Fourier transforms of each other;	

What can the **coherent** and **incoherent** J/ψ photoproduction at $x \sim 0.01$ tell us?



Ultra-Peripheral Collisions at RHIC

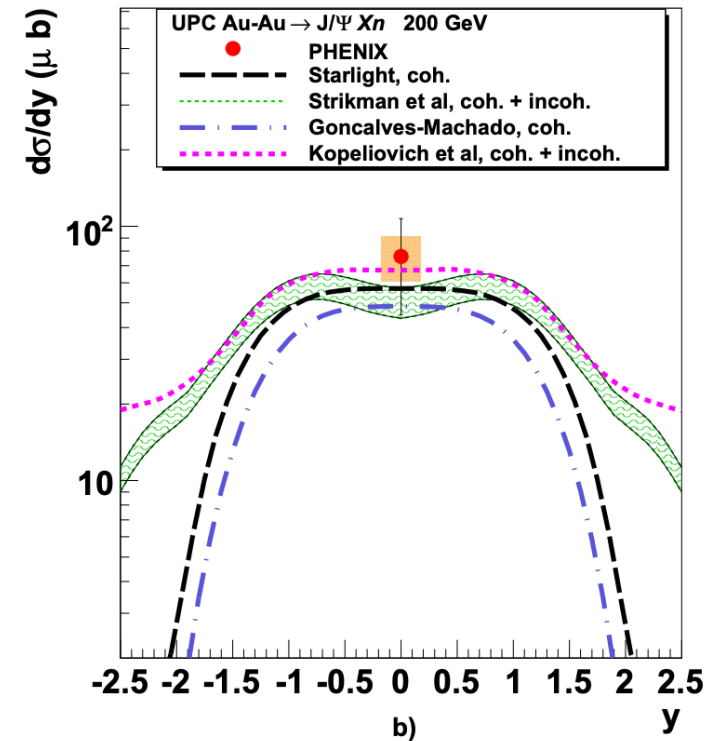
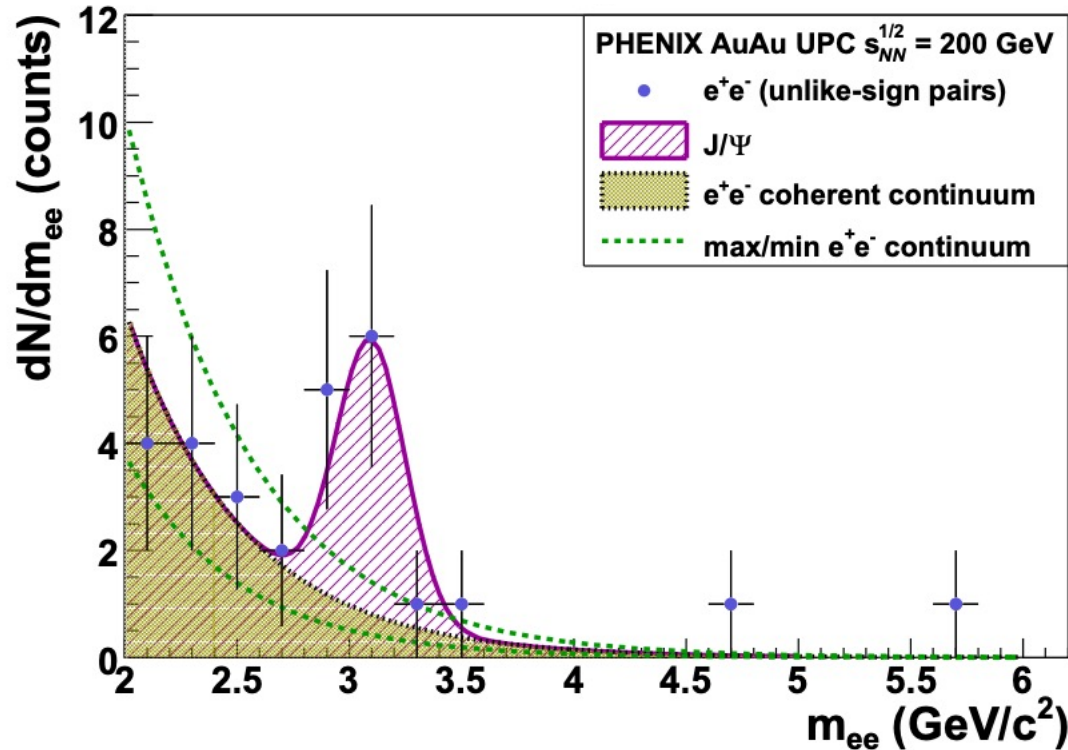


U^{238} , Au^{197} , Zr^{96} , Ru^{96} , d^2 at 200 GeV and pp at 510 GeV

A versatile program with different species, energy, and polarization.



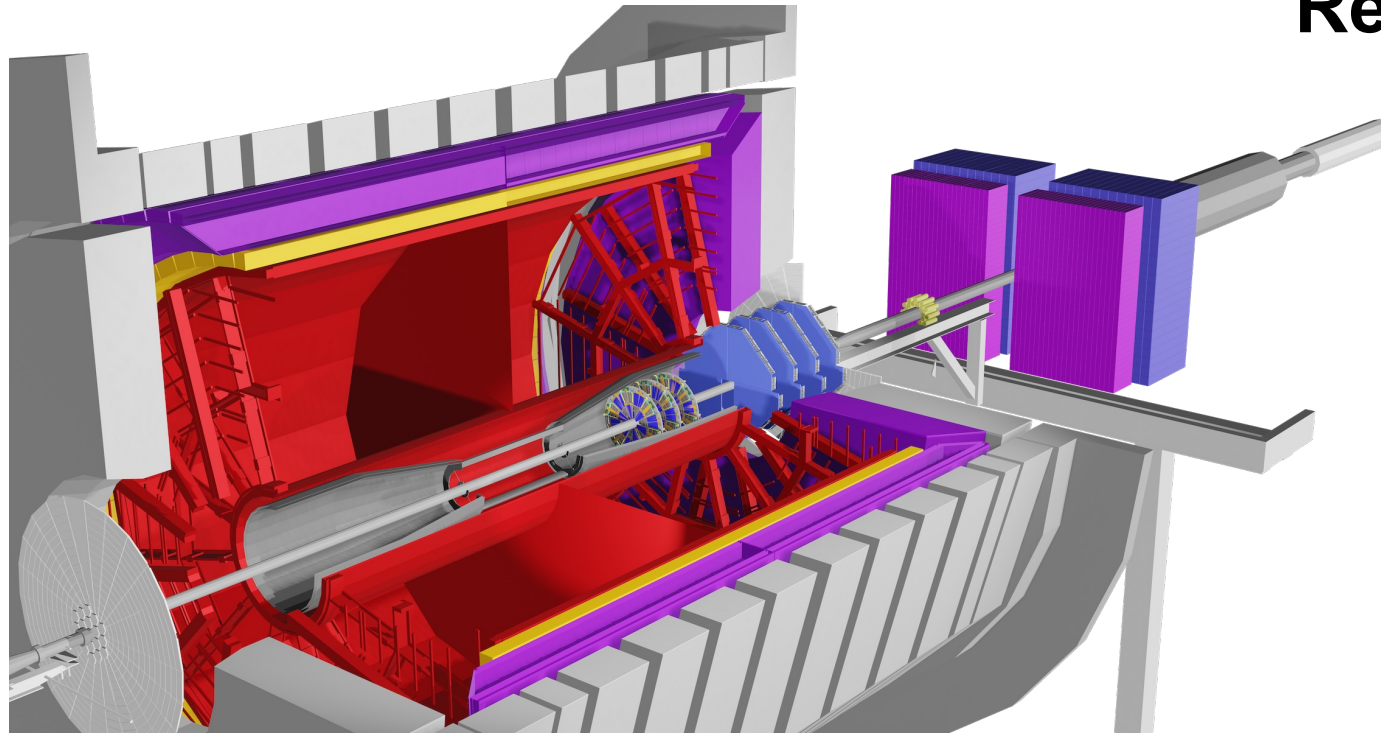
Early RHIC data from PHENIX *Phys. Lett. B 679 (2009) 321-329*



Statistics was limited, coherent and incoherent were not separated, and with neutron selections



STAR experiment



Relevant central detectors

Time Projection Chamber
(TPC)

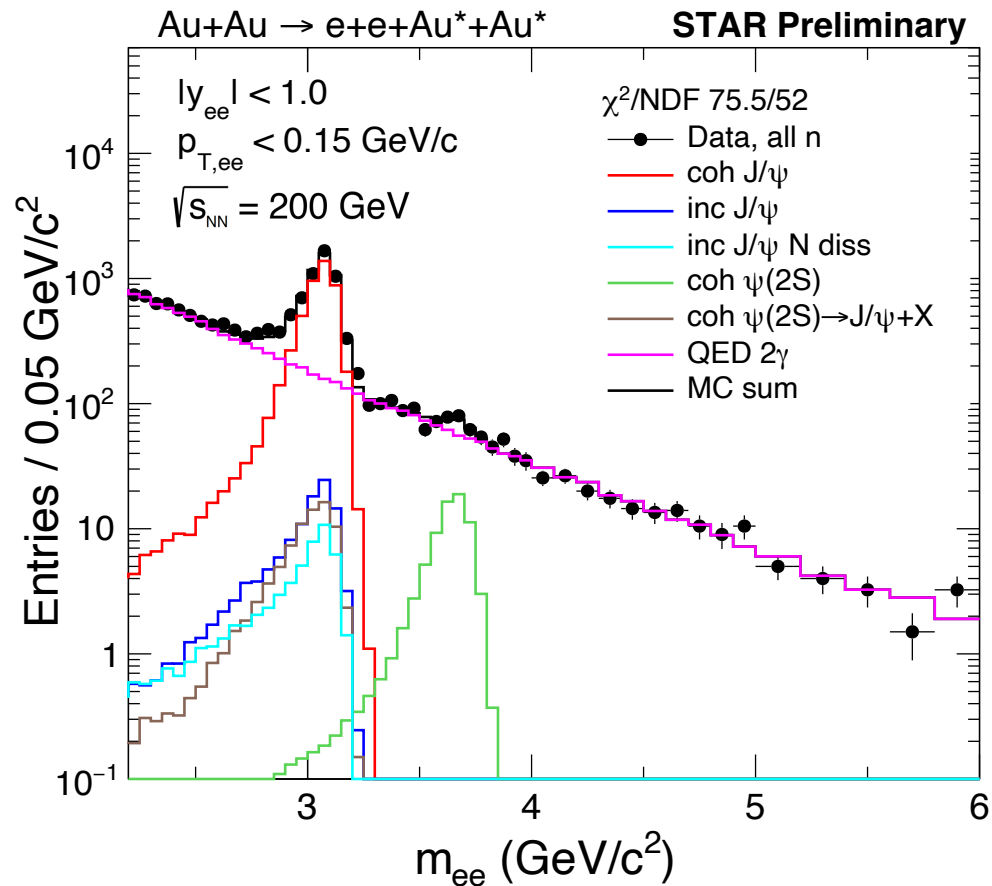
Time-Of-Flight detector
(TOF)

Barrel EM Calorimeter
(BEMC)

Since 2022, STAR has forward detectors ($2.5 < \eta < 4.0$), which would be crucial to the RHIC Run 23-25 physics program



Measuring J/ψ in 200 GeV Au+Au UPCs



Data analysis:

$J/\psi \rightarrow e^+e^-$

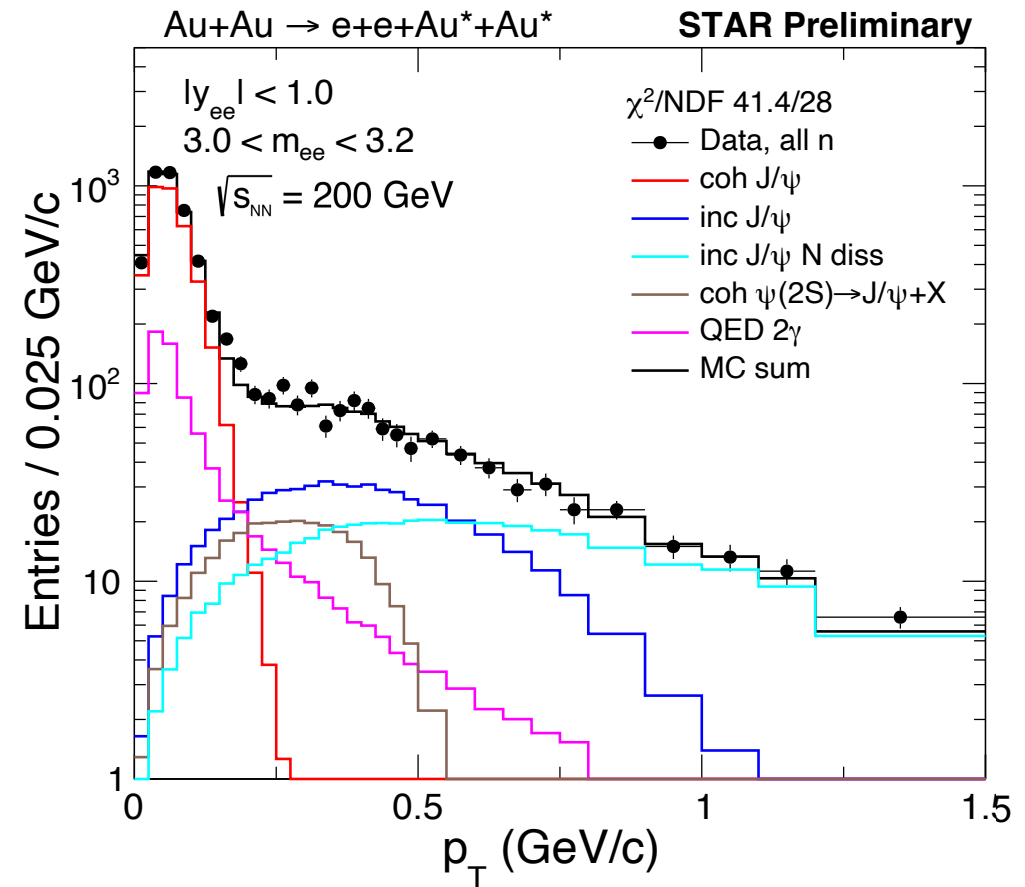
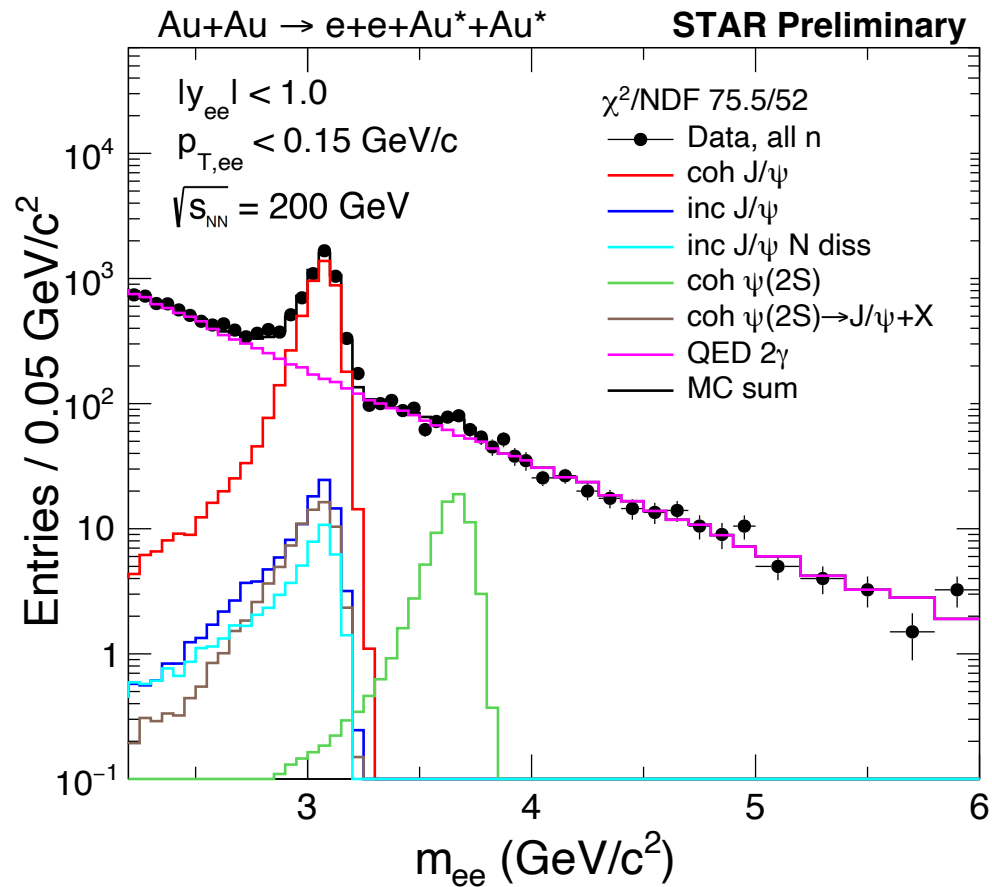
($|y| < 1.0$ for J/ψ , electrons within $|\eta| < 1.0$)

STAR PID (e.g., TPC, TOF) capability
ensures high purity of electron candidates.

Different templates from STARLight and H1
 ep data are used to describe the signal and
backgrounds.



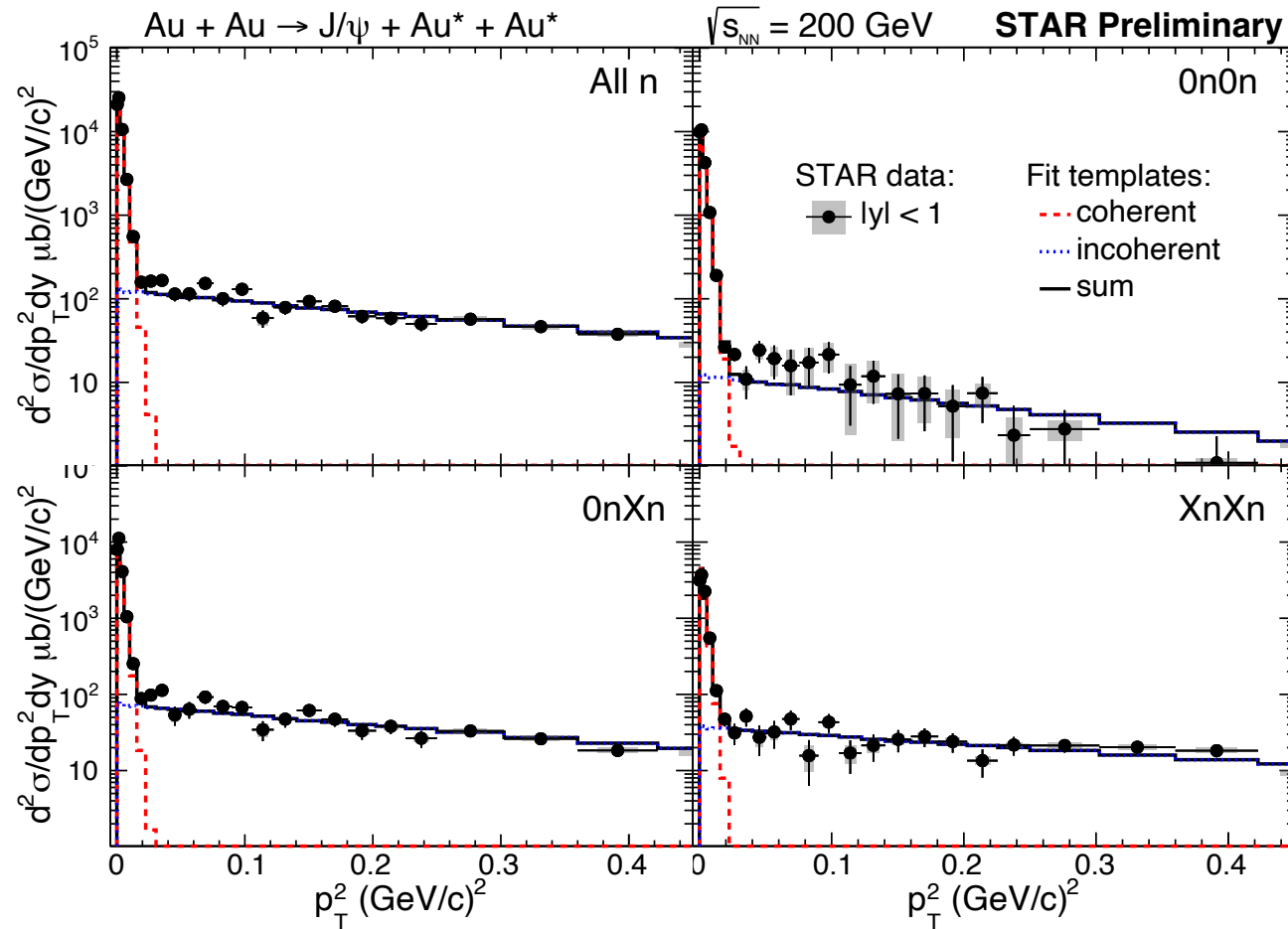
Measuring J/ψ in 200 GeV Au+Au UPCs



when $Q^2 \sim 0$, p_T of J/ψ is directly related to momentum transfer ($t \sim p_T^2$)



Separating coherent and incoherent J/ψ

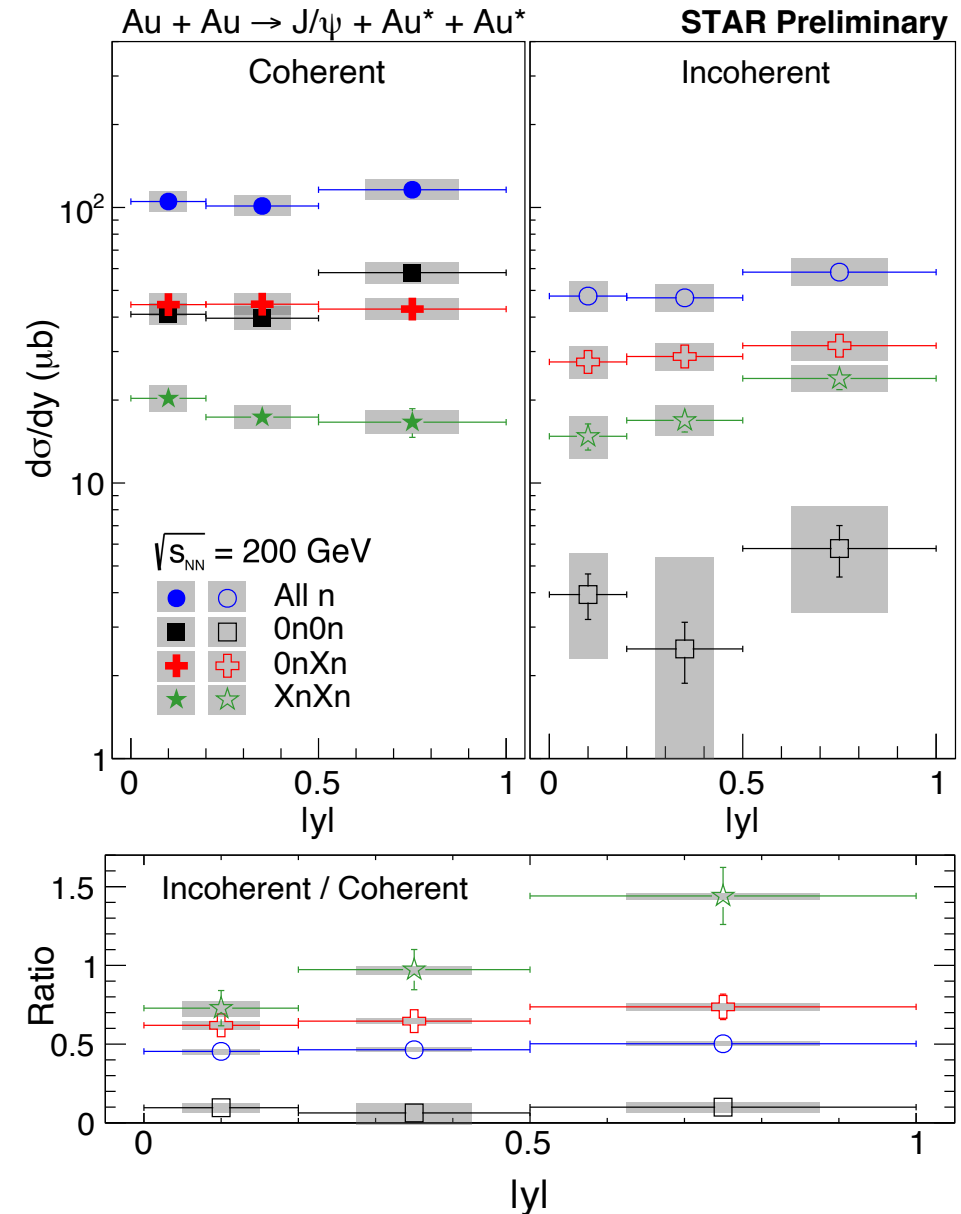


- Low momentum transfer (p_T^2) is dominated by **coherent** photoproduction.
- For incoherent production at low p_T^2 , it is extrapolated using different templates.
- These differences, however, are small to the total incoherent production cross section.



First measurement of y -dependence of J/ψ at RHIC

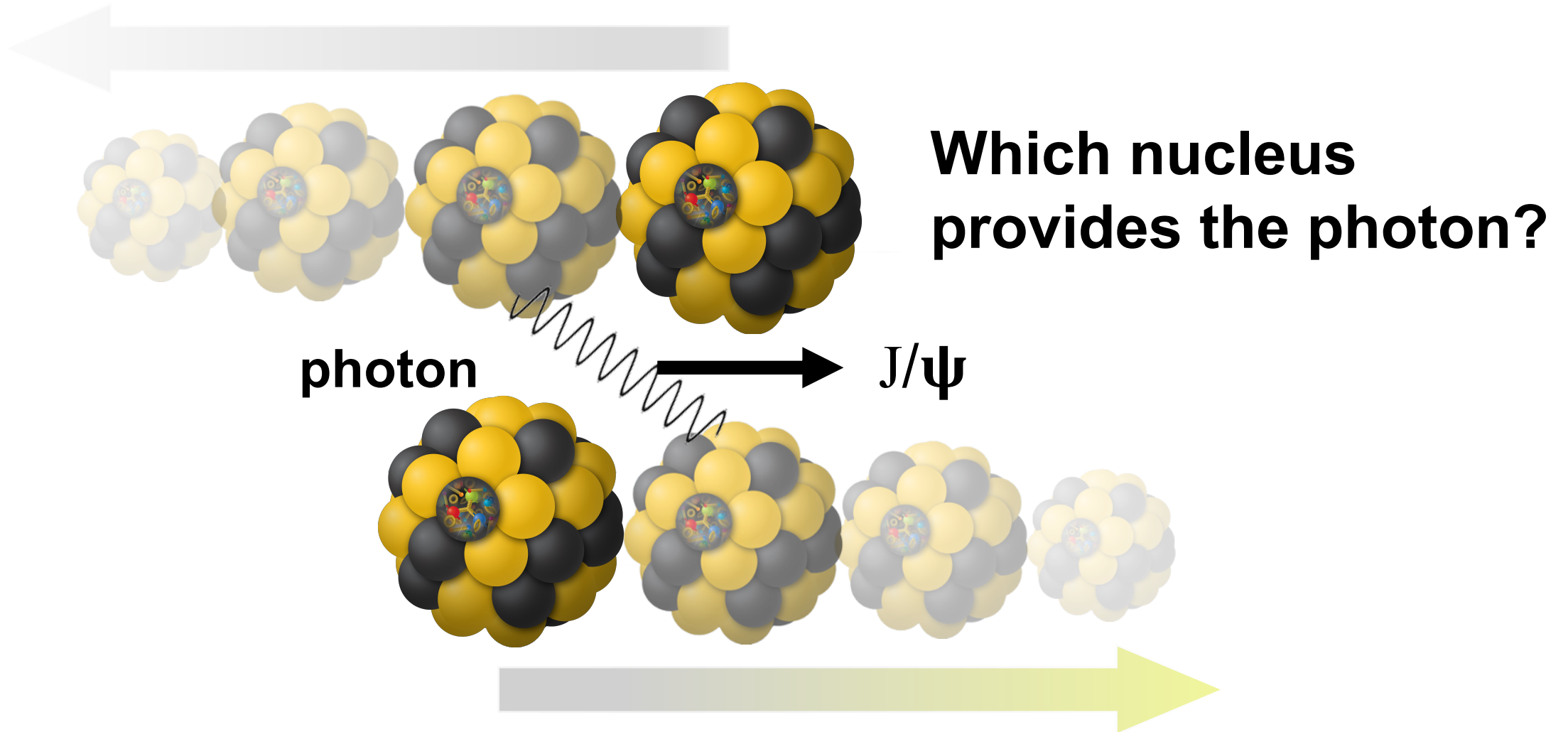
- ❖ Important measurements to constrain theoretical models
- ❖ Ratio of incoherent to coherent cross section largely cancels uncertainties both experimentally and theoretically
- ❖ New studies show this ratio is sensitive to nuclear structure and nuclear deformation (by [W. Zhao et al.](#) at a recent INT workshop)



New

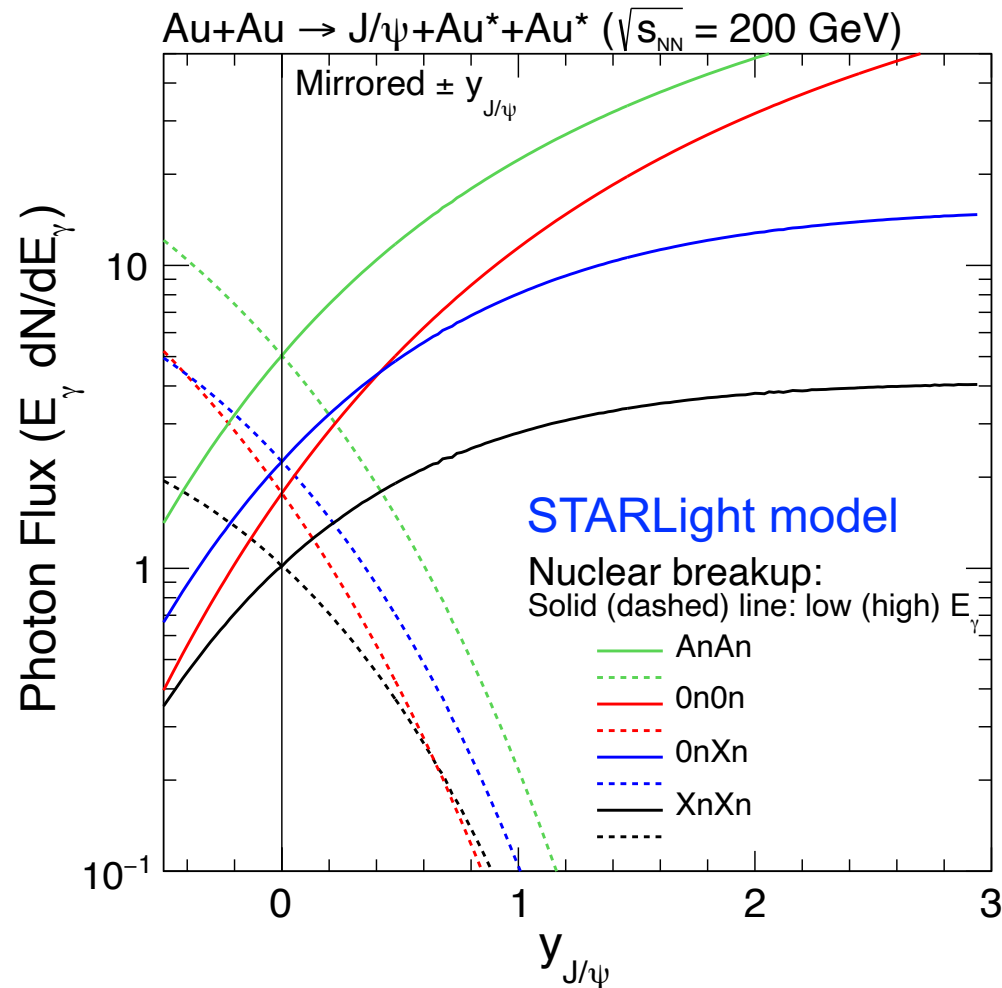


AuAu UPCs: two-source ambiguity





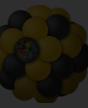
Photon flux and neutron emissions for coherent J/ψ



- If VM at rapidity $y \neq 0$, there is a high energy photon (k_1) candidate and a low energy photon (k_2) one;
- Different photon energies correspond to different flux factors (\sim number of photons)
- Different neutron emission classes associate with different flux factors

Neutron classes:

- **0n0n**: no neutron on either side
- **0nXn**: ≥ 1 neutron on one side
- **XnXn**: ≥ 1 neutron on both sides



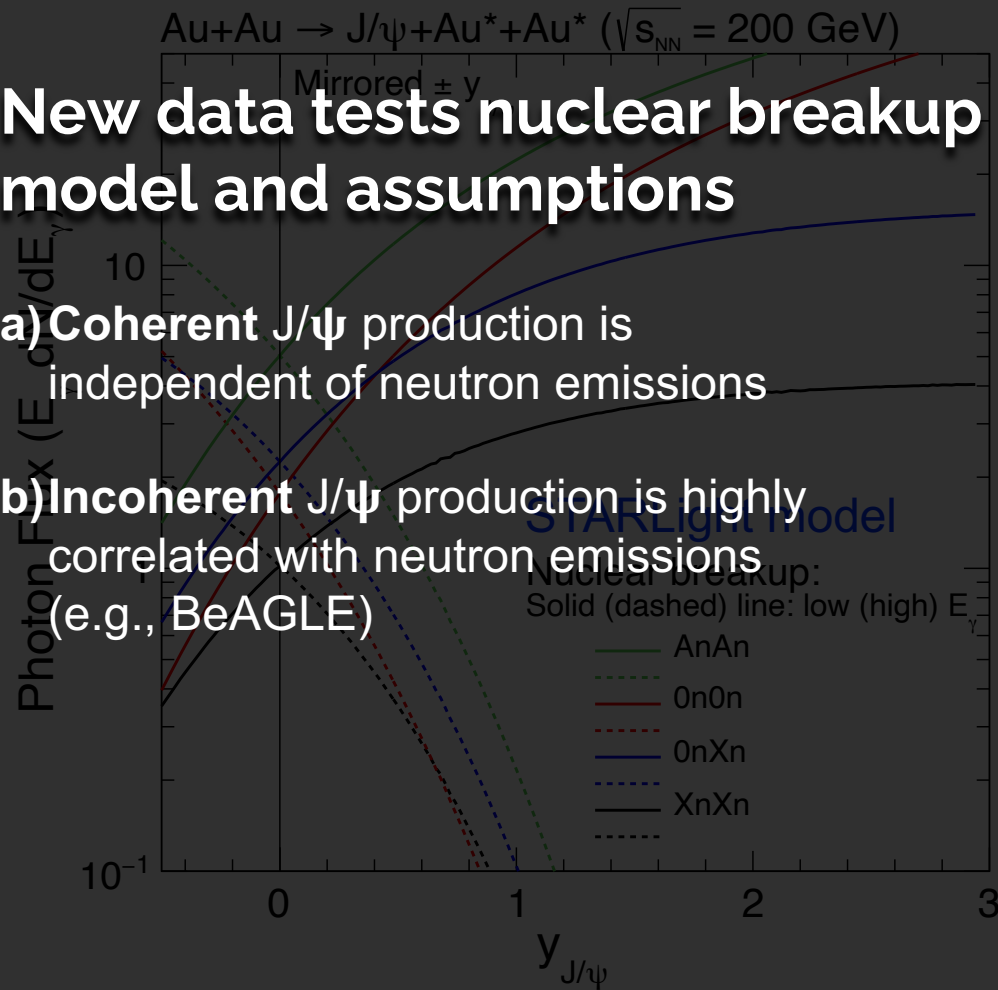
Photon flux and neutron emissions

New

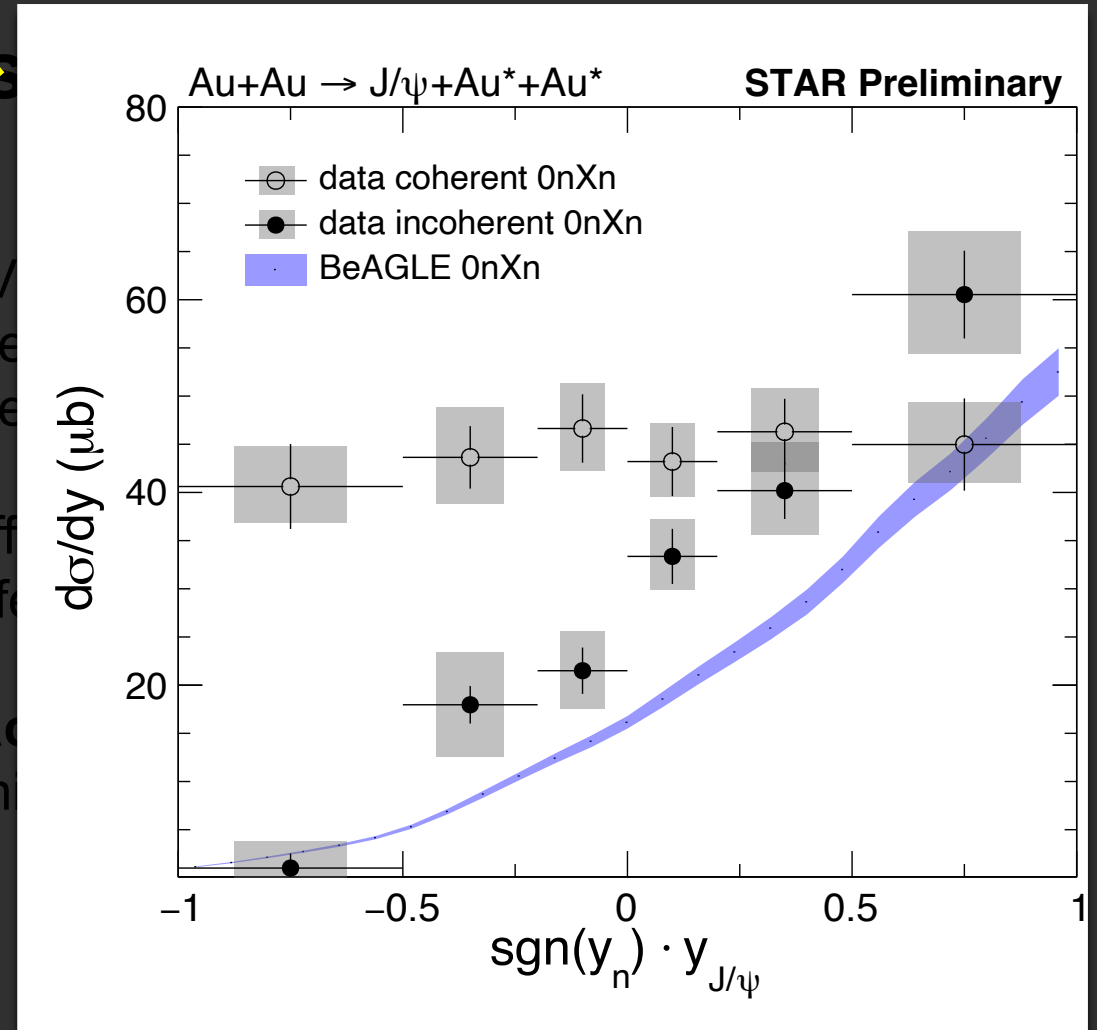
New data tests nuclear breakup model and assumptions

a) Coherent J/ψ production is independent of neutron emissions

b) Incoherent J/ψ production is highly correlated with neutron emissions (e.g., BeAGLE)



- If V ene ene
- Diff diff
- Eac em



• XnXn: ≥ 1 neutron on both sides

Reference to BeAGLE: *Phys. Rev. D* 106 (2022) 1, 012007



Neutron emission helps resolve the two-source ambiguity

$$d\sigma^{AnBn}/dy = \Phi_{T.\gamma}^{AnBn}(k_1) \sigma_{\gamma^* + Au \rightarrow J/\psi + Au}(k_1) + \Phi_{T.\gamma}^{AnBn}(k_2) \sigma_{\gamma^* + Au \rightarrow J/\psi + Au}(k_2)$$

Measurements (slide 12)

Photon fluxes (slide 14)

Unknowns

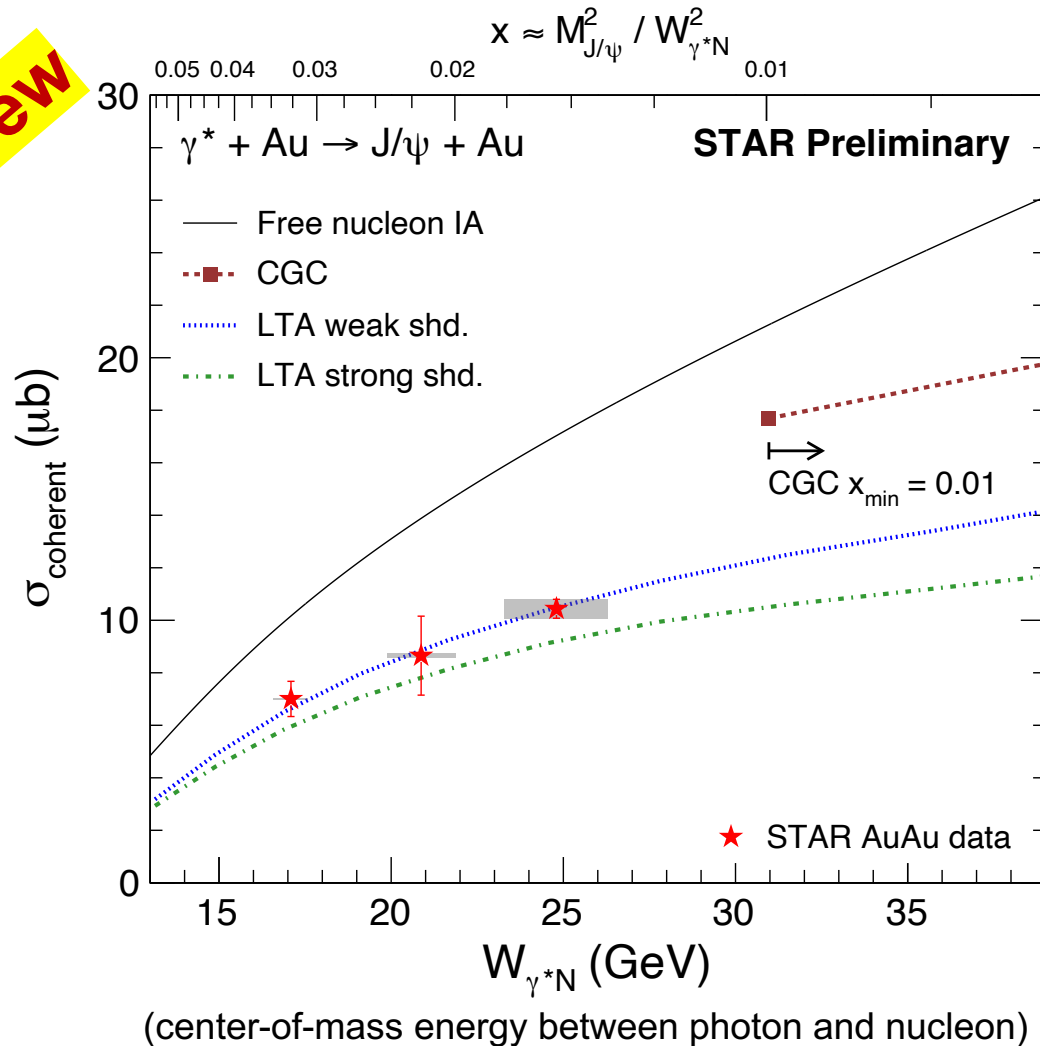
Eur. Phys. J C (2014) 74:2942

Need to measure differential cross section in y and in neutron emission classes; **at least 2 equations to solve 2 unknowns.**



Coherent J/ψ cross section vs energy W

New



- ❖ STAR kinematics is unique to the low W region, while gluon saturation models generally focus on higher energy.
- ❖ Shadowing model LTA describes the data very well. **The suppression factor (data/IA) is ~ 60%**
- ❖ Sensitive to the transition region between high- x and low- x .

Reference to CGC: *Phys. Rev. D* 106 (2022) 7, 074019

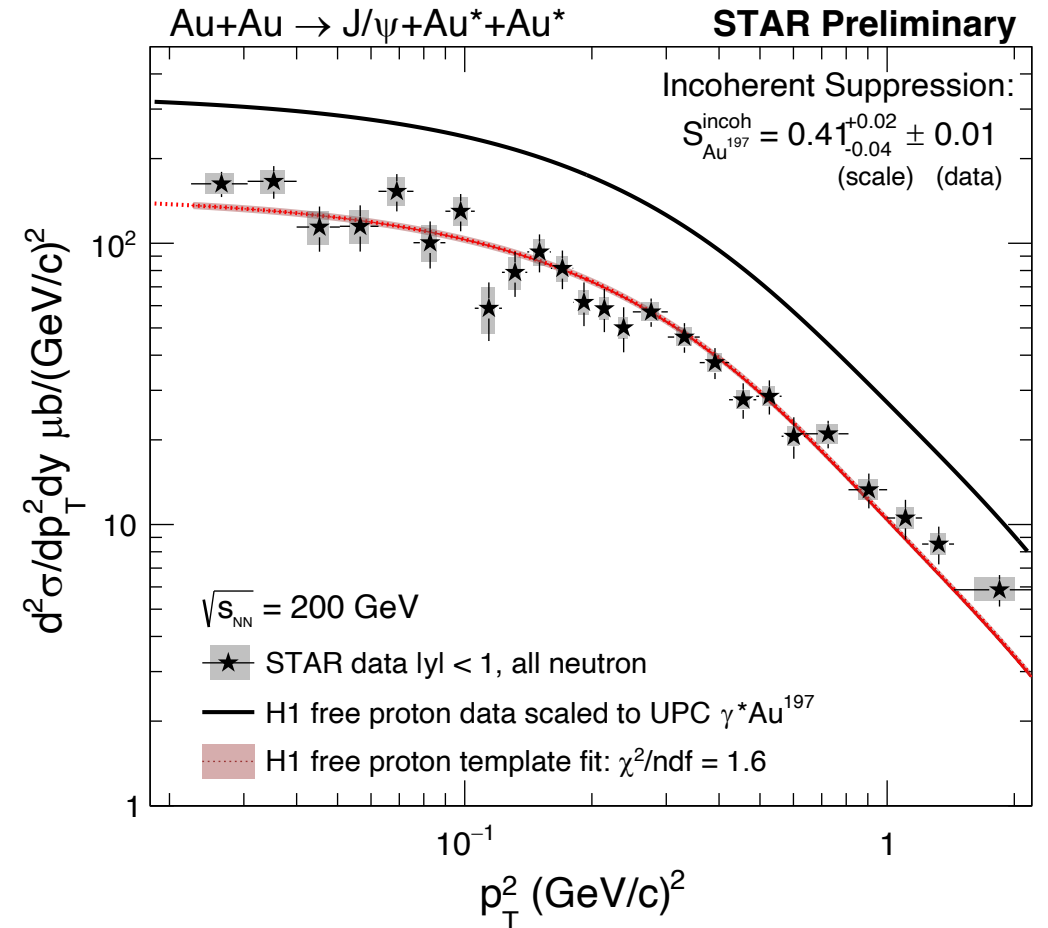
Reference to LTA: 1) Guzey, Strikman, Zhalov, EPJC 74 (2014) 7, 2942 2. Strikman, Tverskoy, Zhalov, PLB 626 (2005) 72-79



Incoherent J/ψ cross section vs p_T^2

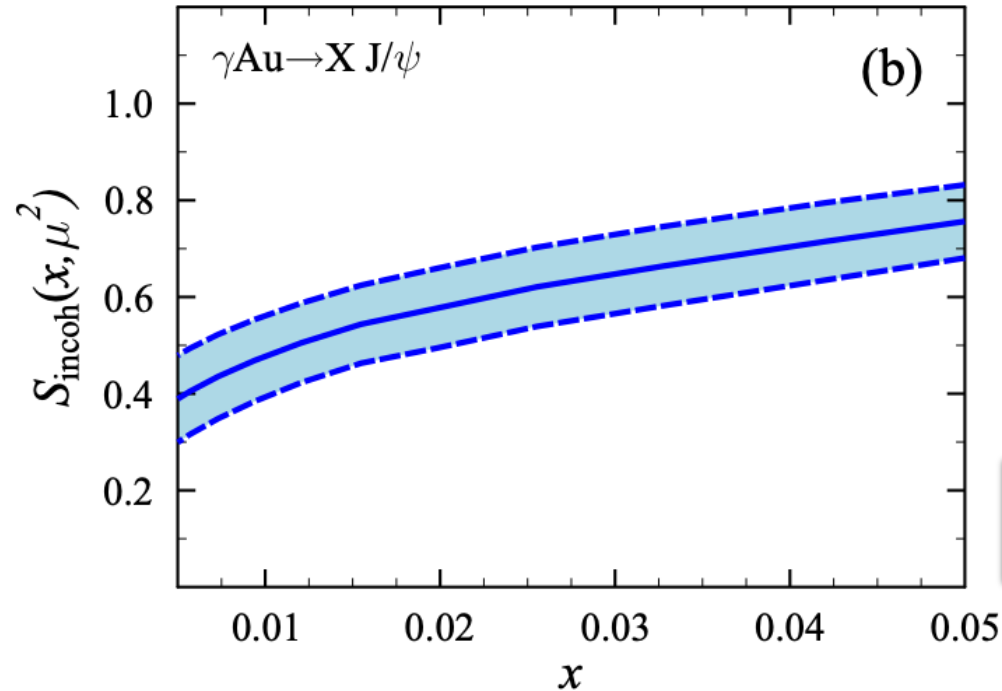
New

- ❖ Compared to the H1 data with free proton.
The suppression factor ~ is 40%.
 Stronger than that for coherent production.





Shadowing in incoherent J/ψ photoproduction



This ratio is driven by multi-nucleon interactions, nuclear thickness function, diffractive parton distributions, etc.

(Phys. Rev. C 108 (2023) 2, 024904)

$$S_{\text{incoh}}(x, \mu^2) = \frac{1}{A} \int d^2\mathbf{b} T_A(\mathbf{b}) \left[1 - \frac{\sigma_2(x, \mu^2)}{\sigma_3(x, \mu^2)} \left[1 - e^{-\frac{\sigma_3(x, \mu^2)}{2} T_A(\mathbf{b})} \right] \right]^2 .$$

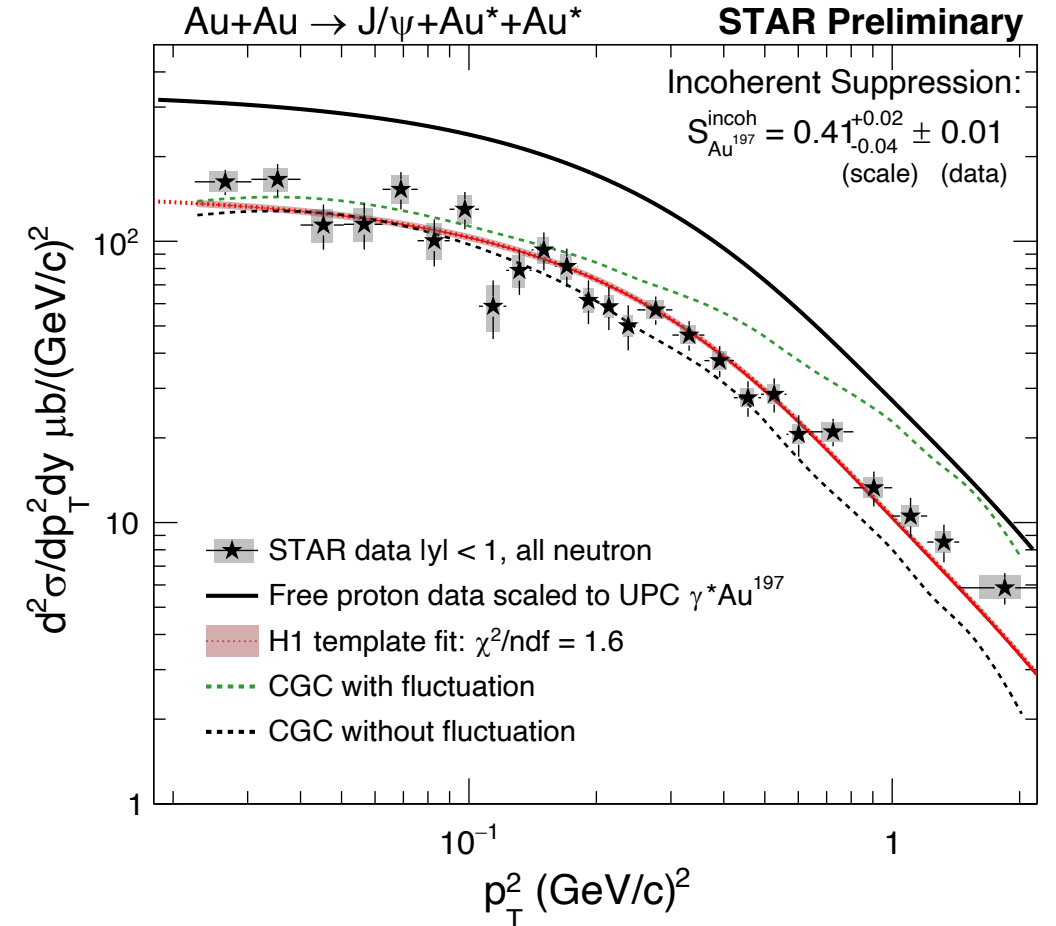
Intuitively, the incoherent J/ψ production is the convolution of: J/ψ production off a nucleon inside of a nucleus \otimes probability of the J/ψ survives on its way out of the nucleus.



Incoherent J/ψ cross section vs p_T^2

New

- ❖ Compared to the H1 data with free proton. **The suppression factor ~ is 40%.** Stronger than that for coherent production.
- ❖ Models have found that the H1 data supports **sub-nucleonic fluctuation**.
[*Phys. Rev. Lett.* 117 (2016) 5, 052301]
- ❖ STAR data shows the bound nucleon has a similar shape in p_T^2 as the free proton, indicating **similar sub-nucleonic fluctuation in heavy nuclei**.
[*Phys. Rev. D* 106 (2022) 7, 074019]

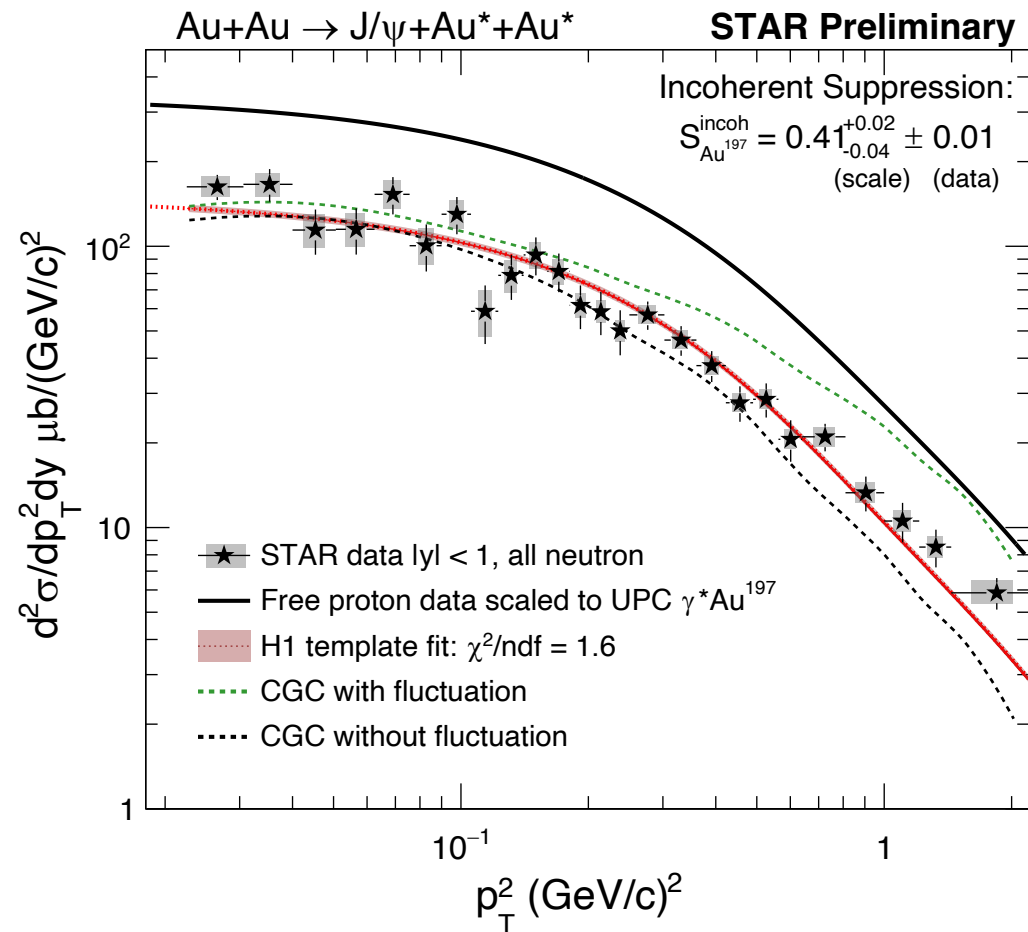
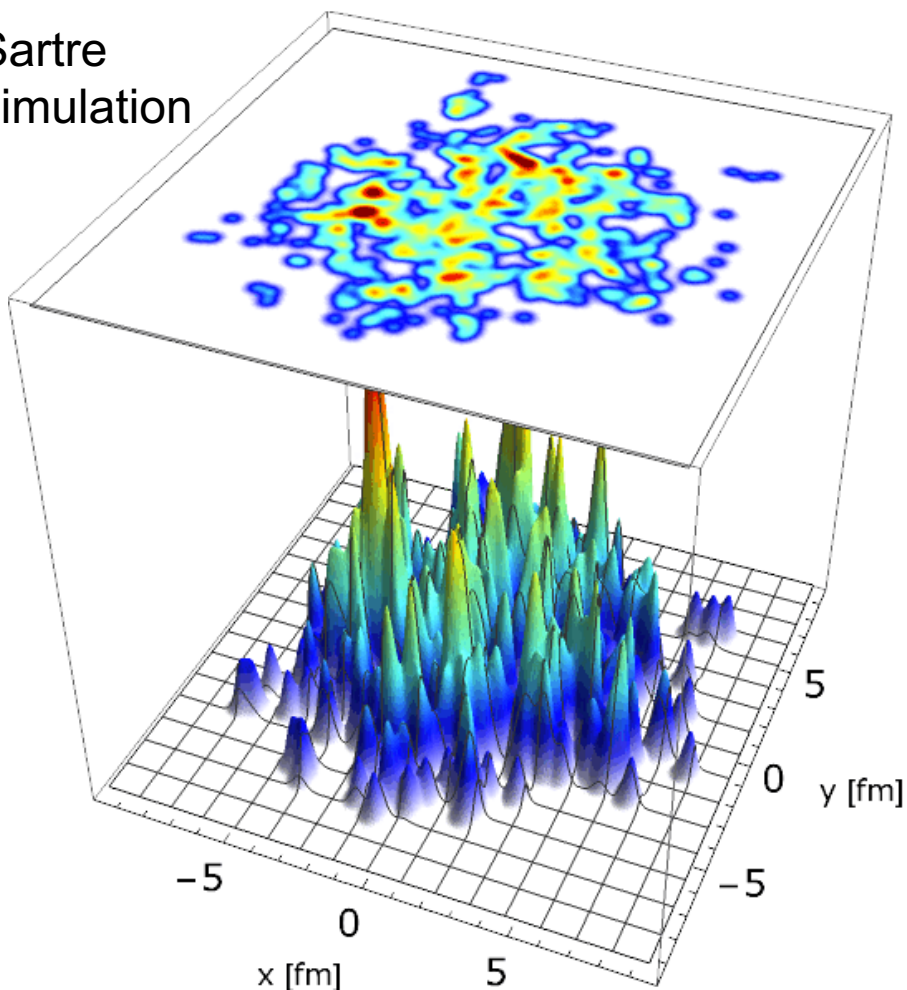




Incoherent J/ψ cross section vs p_T^2

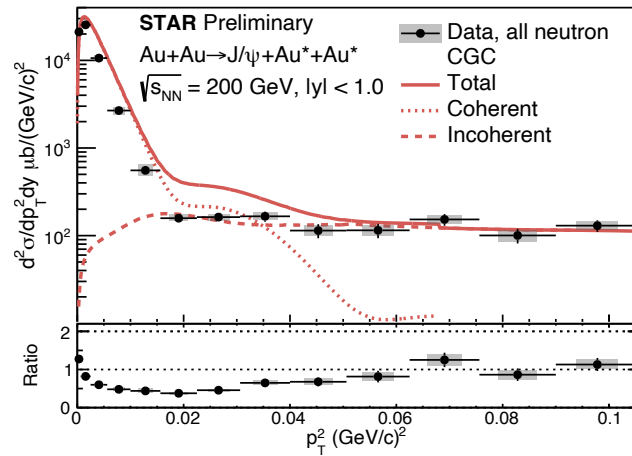
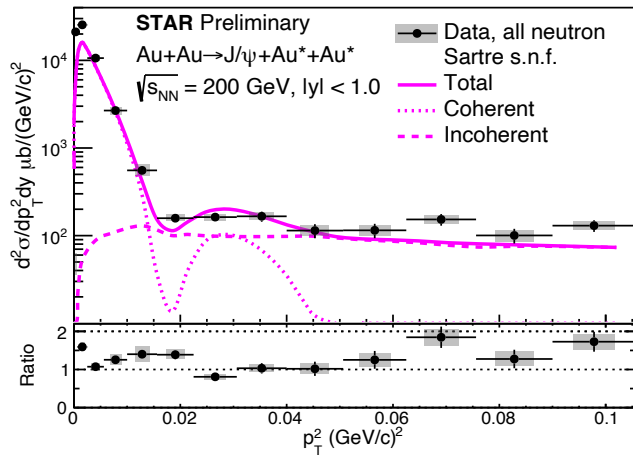
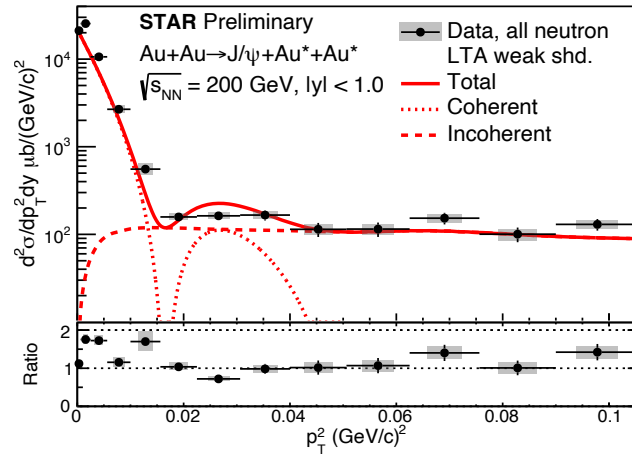
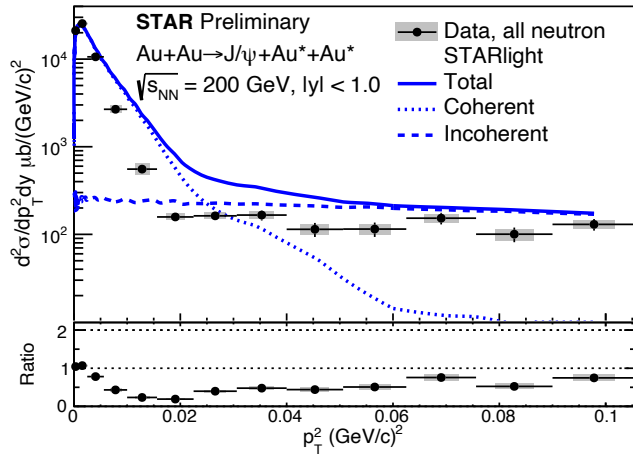
New

Sartre simulation





A full picture: coherent + incoherent



- ❖ STAR data compared with four theory/MC models.
- ❖ Sartre with sub-nucleonic fluctuation (s.n.f) & CGC are similar models but different by a normalization factor ~ 0.65 .
- ❖ Question to theorists: Why?

Reference to CGC: *Phys. Rev. D* 106 (2022) 7, 074019
 Reference to LTA: [arXiv:2303.12052](https://arxiv.org/abs/2303.12052)



NLO calculation

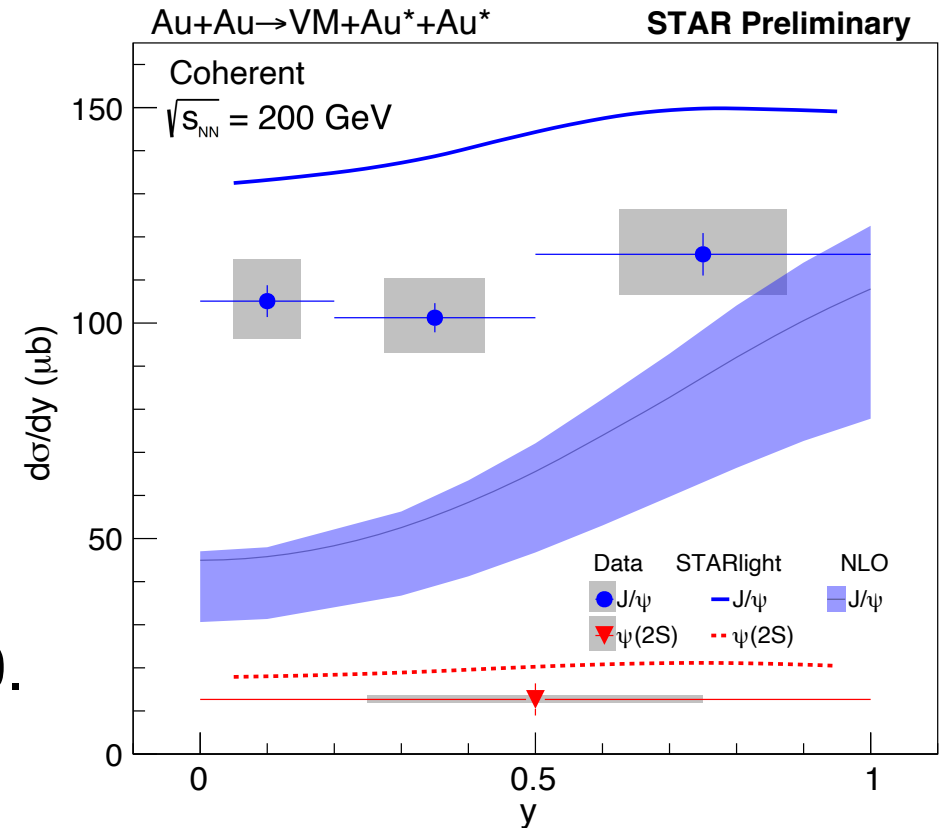
Next-to-Leading Order (NLO) pQCD calculation, constrained by the LHC data

EPPS21 + scale at 2.39 GeV.
Only scale uncertainty shown.

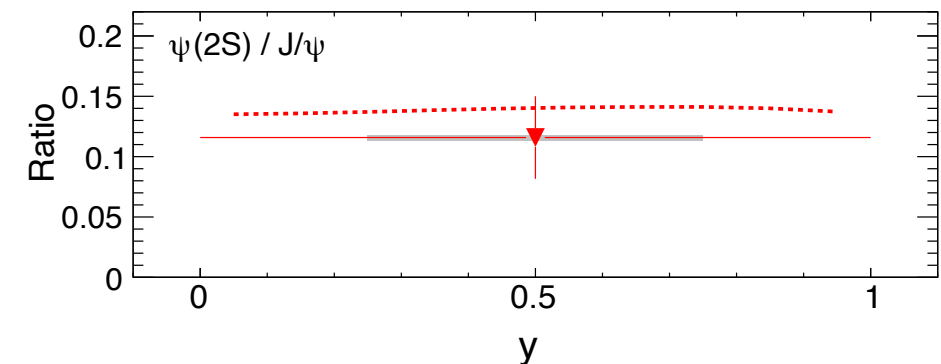
Could not describe the STAR data at $y = 0$.

Reference to NLO pQCD calculation:

- arXiv:2210.16048
- Phys. Rev. C 106 (2022) 3, 035202

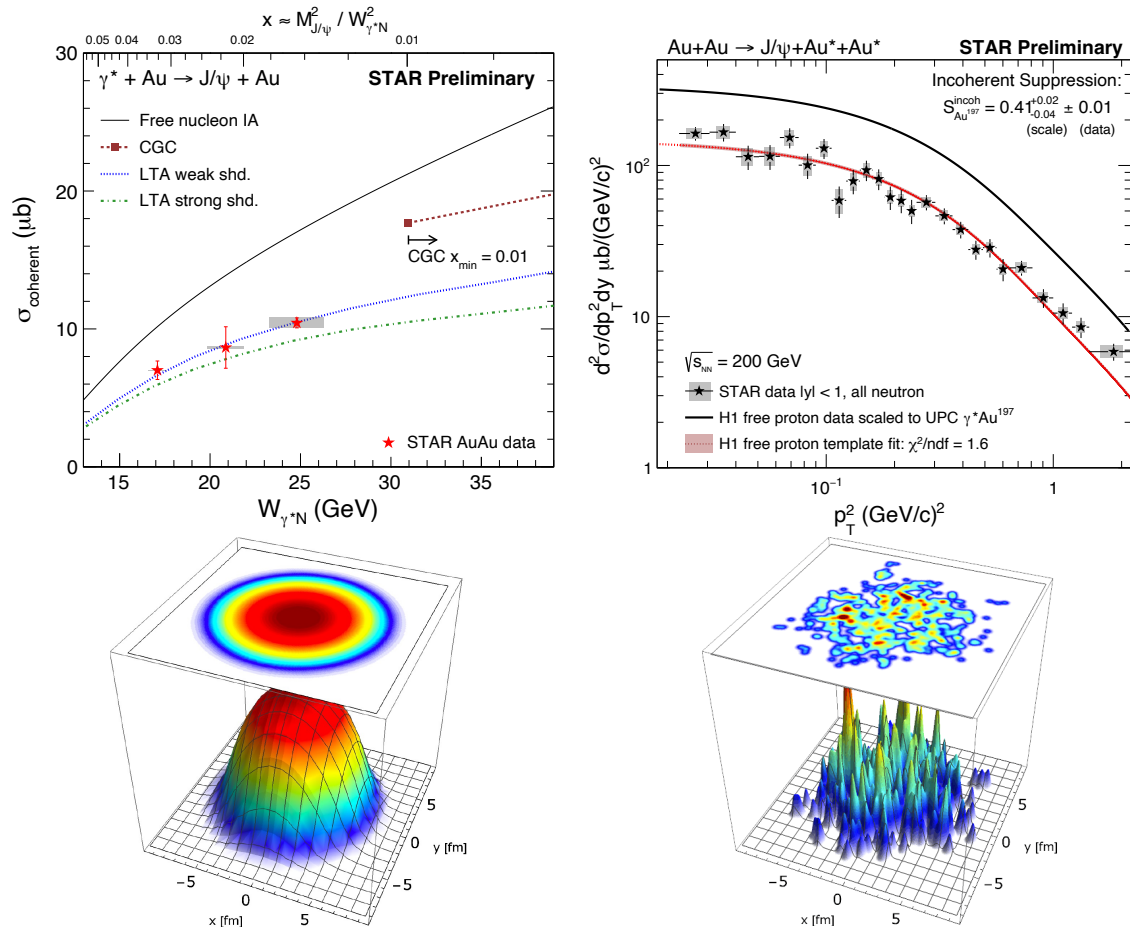


New





Summary – coherent and incoherent J/ψ photoproduction

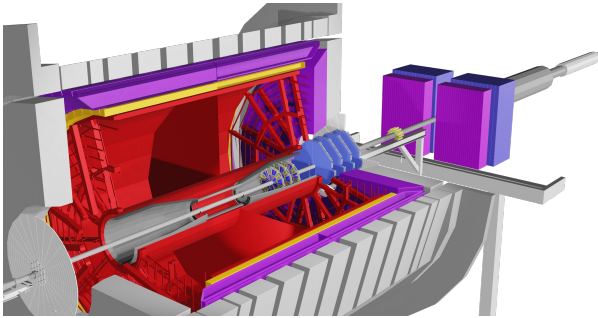


STAR has made many **first-time J/ψ** measurements in UPCs at RHIC:

- ✓ Strong **nuclear suppression** seen for both coherent ($\sim 40\%$) and incoherent ($\sim 60\%$) production.
- ✓ **Bound** nucleon and **free** proton have similar shape in p_T^2 up to $\sim 2.2 (\text{GeV}/c)^2$
- ✓ Coherent is sensitive **average** parton density (or imagining if measure momentum) and Incoherent is sensitive to the parton density **fluctuation**.



Future UPCs opportunities



Since 2022, STAR has forward detectors ($2.5 < \eta < 4.0$):

- J/ψ coherent and incoherent production with **high precision**. Lower W towards a few GeV, and high t to better understand fluctuation.
- ϕ photoproduction.
- Photoproduction of jets.
- **New observables.**

RHIC 23-25

2023

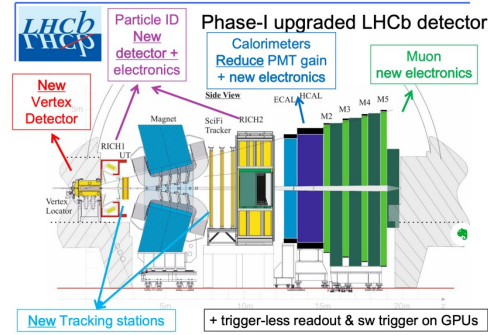
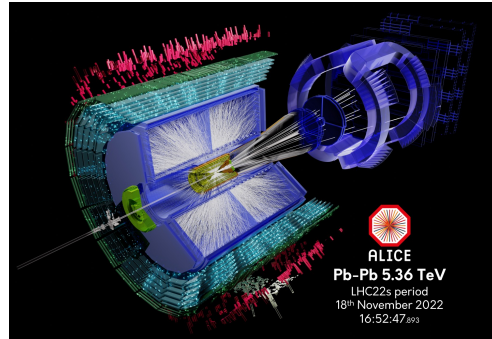
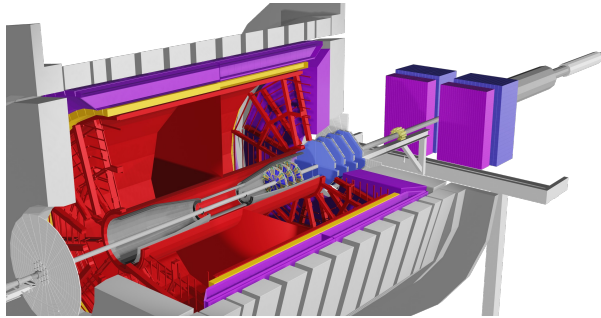
2025

2029

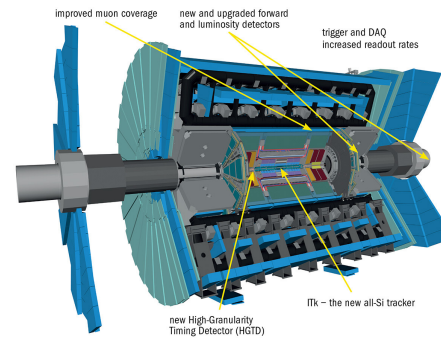
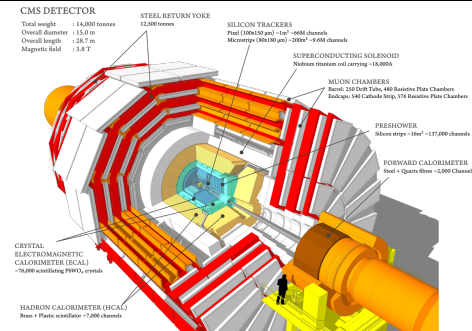
2034+



Future UPCs opportunities



- Since 2022, STAR has forward detectors ($2.5 < \eta < 4.0$):
- J/ψ coherent and incoherent production with **high precision**. Lower W towards a few GeV, and high t to better understand fluctuation.
 - ϕ photoproduction.
 - Photoproduction of jets.
 - New observables.



All LHC experiments will have significant upgrades in Run 3 & 4 (e.g., wide acceptances, ALICE FoCal, etc.). **Lower-x reach!**

RHIC 23-25 & LHC Run 3

LHC Run 4

2023

2025

2029

2034+

Special thanks to:

CGC: Heikki Mäntysaari, Farid Salazar, Björn Schenke

Sartre: Tobias Toll, Arjun Kumar

Nuclear shadowing: Vadim Guzey, Mark Strikman, Mikhail Zhalov

NLO pQCD: Topi Löytäinen et al.

Saturation observables: Brian Sun, Y. Kovchegov

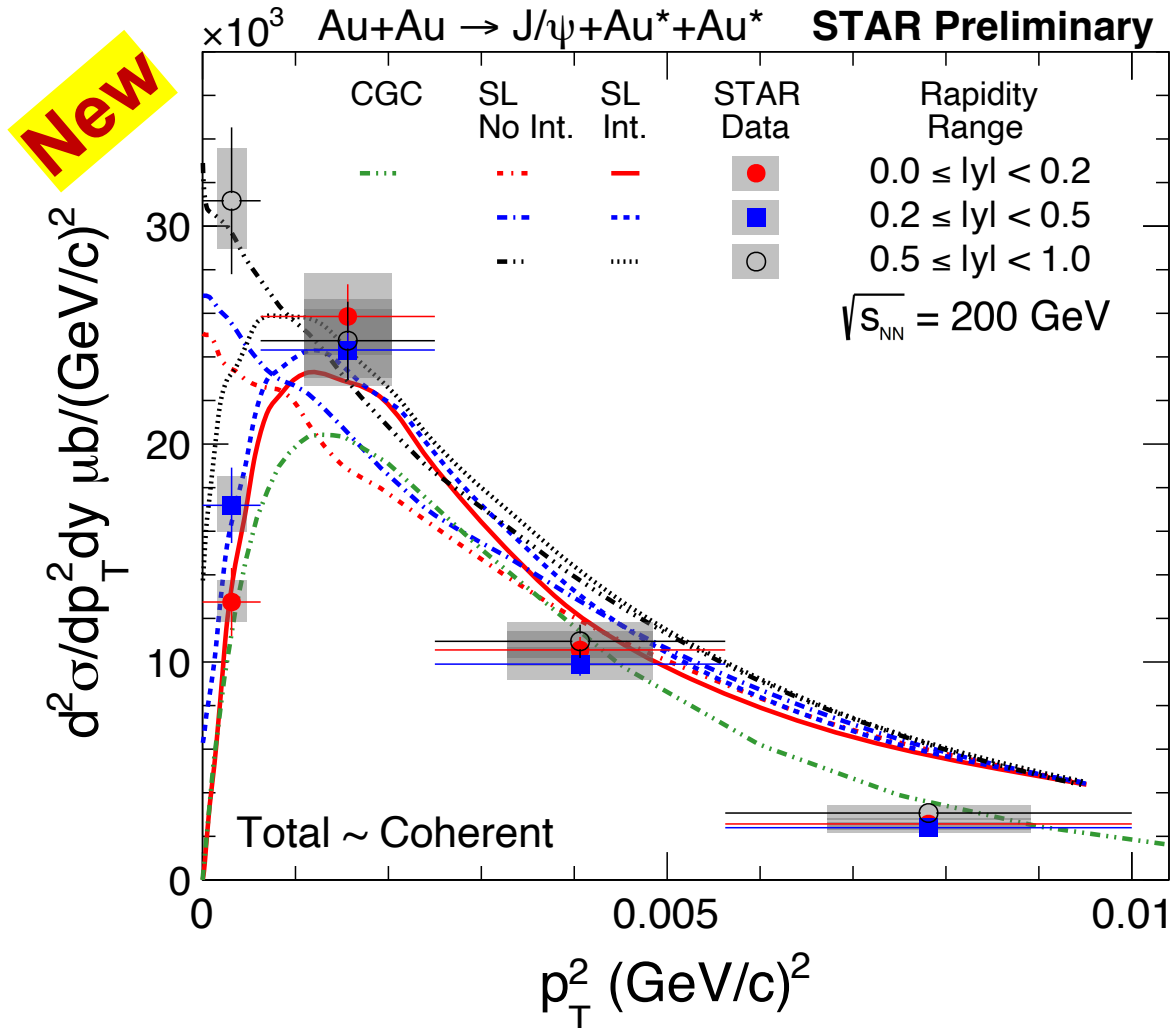
For discussions and inputs.



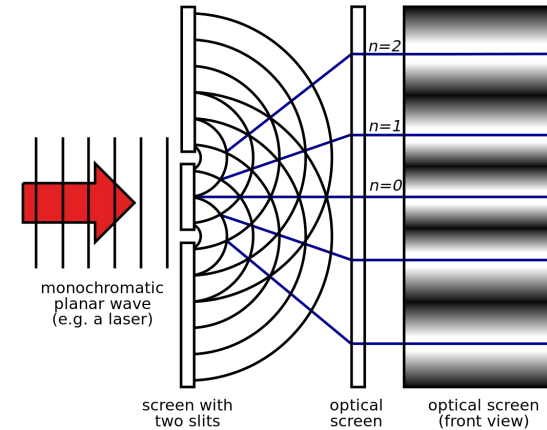
Backup



Two-source interference



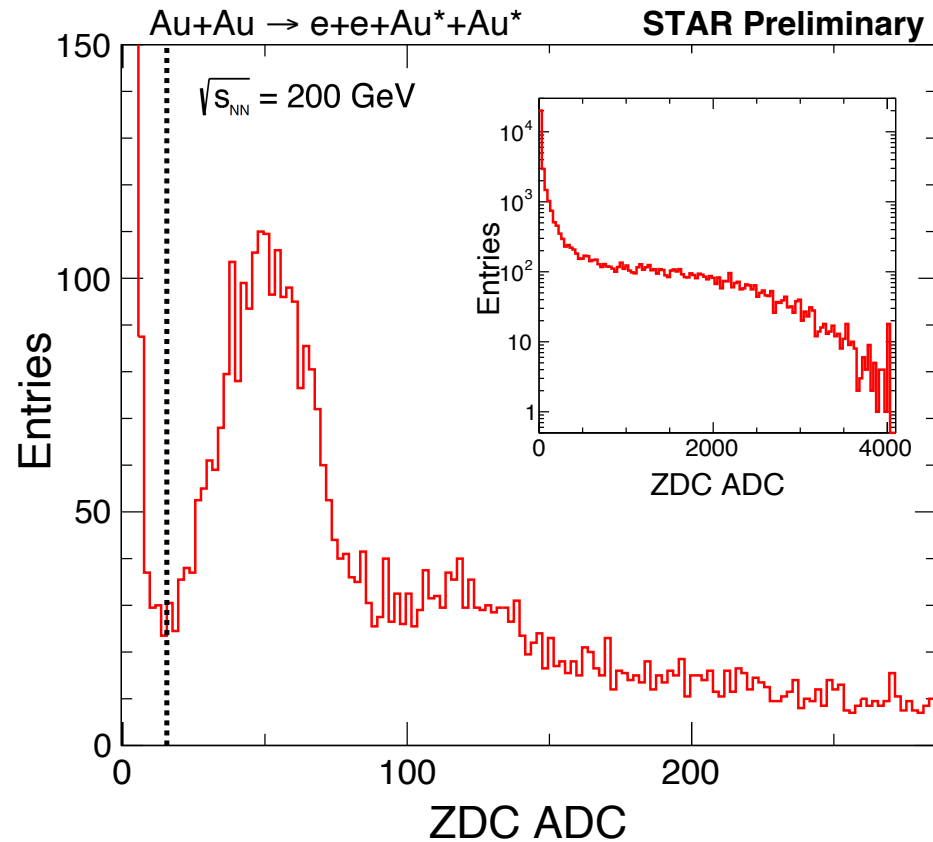
Rapidity dependence is consistent with theory/model; interference effect is stronger if photon energies are similar.



First observed w. ρ^0 in 2008 by STAR (Phys.Rev.Lett.102:112301,2009)

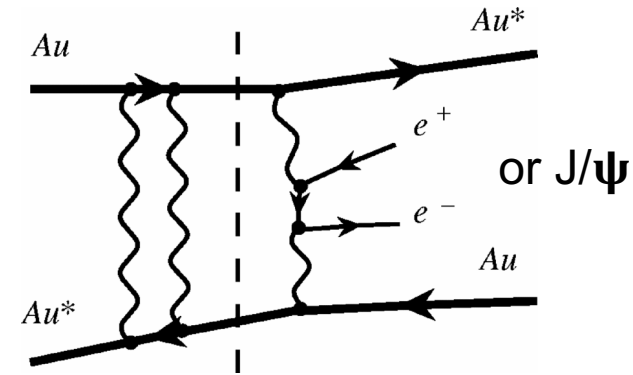


Neutron emissions in UPCs

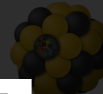


Neutron classes:

- **0n0n**: no neutron on either side
- **0nXn**: ≥ 1 neutron on one side
- **XnXn**: ≥ 1 neutron on both sides



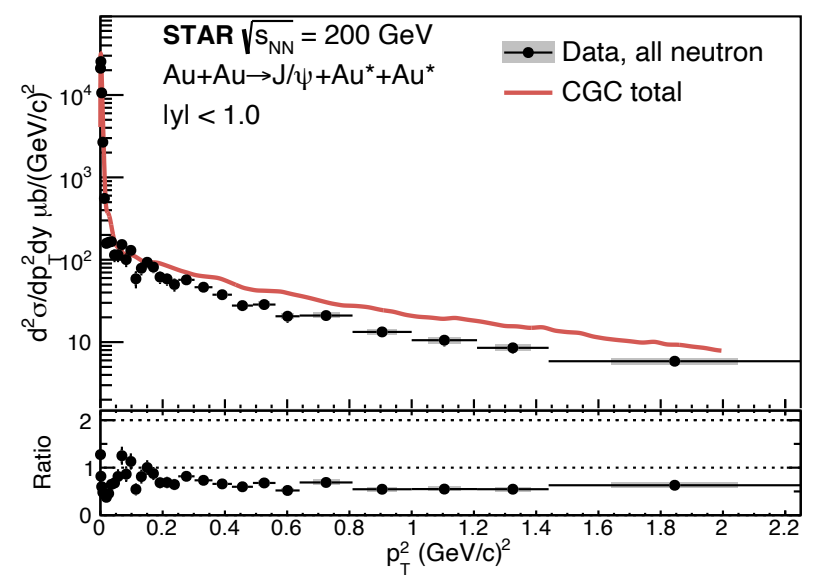
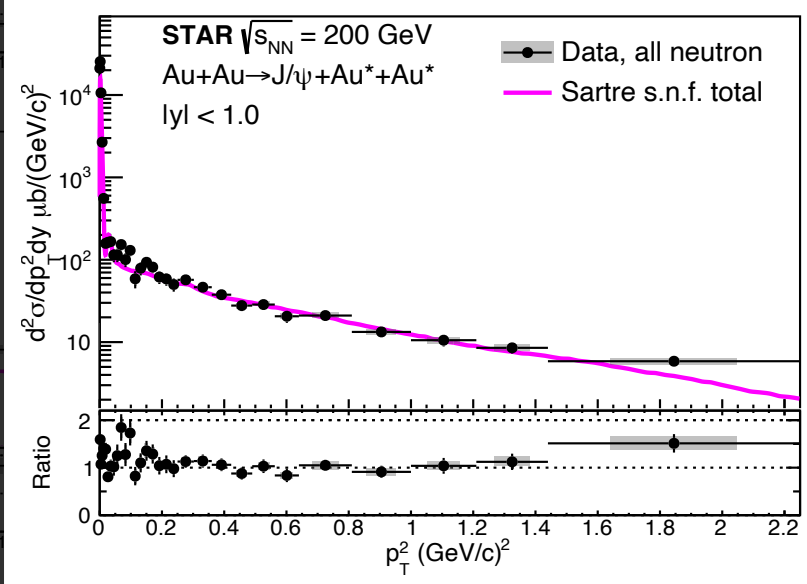
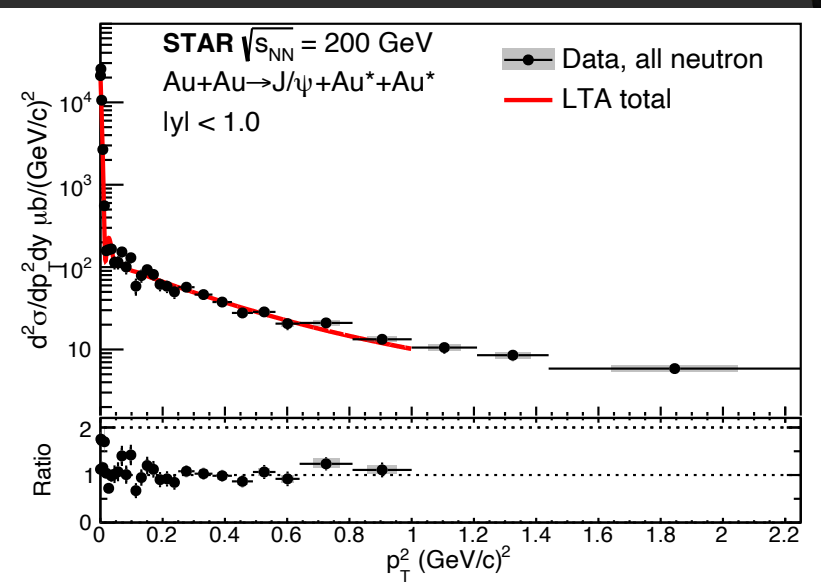
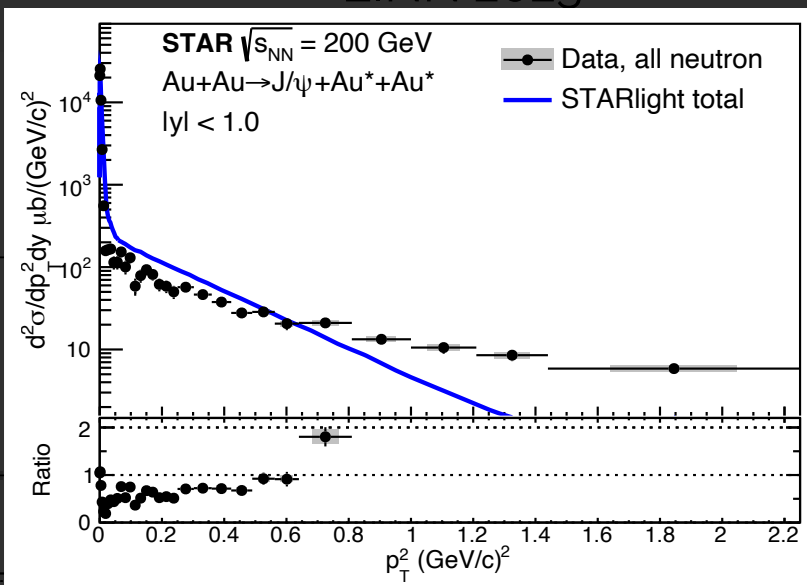
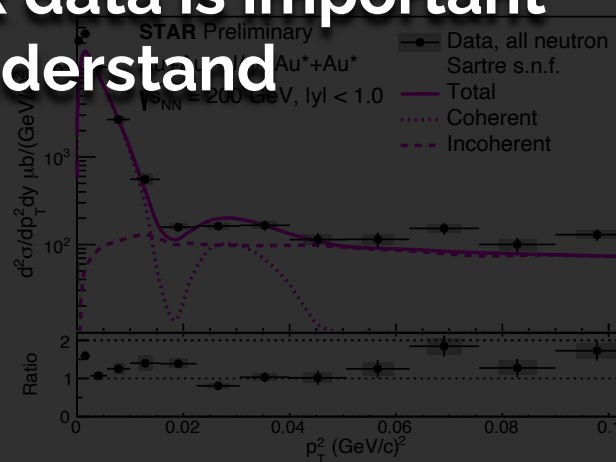
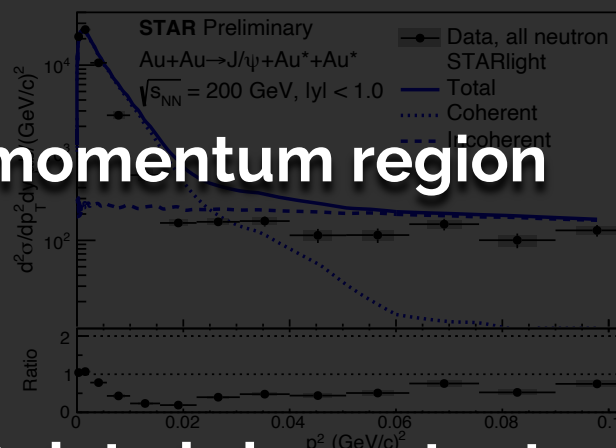
UPCs have large contributions from QED Coulomb excitations



A full picture:

Full momentum region

STAR data is important to understand





Comparison to CGC

